

Plasma resonance in granular deposits and rough surfaces of magnesium

G. Rasigni, J. P. Palmari, and M. Rasigni

Centre d'étude des couches minces, Département de Physique des interactions photons-matière, Faculté des Sciences, Place Victor-Hugo, 13003 Marseille, France

(Received 8 May 1974)

An optical study was made of granular deposits and rough surfaces of magnesium, prepared under ultrahigh vacuum, between 1 and 6 eV. The structure of these deposits was determined *in situ*, using replication techniques. It was shown that discontinuous deposits display plasma resonances of conduction electrons for $\hbar\omega \leq 5.12$ eV. Continuous rough deposits do not exhibit these resonances but show a substantial dip in the reflectance at an energy close to that of the surface-plasmon energy. This dip was explained by means of Elson and Ritchie's quantum theory on the influence of roughness on scattering.

I. INTRODUCTION

When an electromagnetic wave reaches a metal that has the ideal arrangement of ionic cores surrounded by electrons, it generally undergoes an absorption. Depending on the spectral region considered, the theoretical interpretation of this absorption may be made to comply either with Drude's theory or with that of energy bands. By means of a simple theory, we can express the optical conductivity of a metal as the sum of an intraband term (Drude term) $\sigma_D(\omega)$ and an interband term $\sigma_I(\omega)$,

$$\sigma(\omega) = \sigma_D(\omega) + \sigma_I(\omega). \quad (1)$$

Many studies have been centered on determinations of the conductivity and dielectric constant of metals, with a view to testing these hypotheses and gaining a better understanding of structure. Generally, these determinations were effected with thin deposits, and measurements were photometric and polarimetric. It was always assumed that the deposits were limited by two plane parallel faces, separated by a thickness d . In practice, this ideal model is never realized. Generally, the thinnest deposits are granular, and continuous deposits often exhibit surface roughness. An optical study of these deposits revealed two interesting phenomena.

First, as is well known, small-metallic-particle systems exhibit a strong characteristic absorption peak which does not occur in the bulk metal. In suspensions of gold, silver, and sodium colloidal particles the absorption peaks generate beautiful colors. These peaks are due to collective oscillations of conduction electrons, and since 1902 (Wood's¹ pioneer studies) numerous investigations have been made of the optical properties of noble- and alkali-metal particles dispersed in dielectrics, or in island film structures.²⁻¹⁰

Second, it is also well known that normally incident photons can excite nonradiative surface plasmons on a rough surface, but not on a perfectly smooth surface. Experimentally, reflectance val-

ues less than those expected for smooth surfaces have occurred for Ag, Al, and Mg.¹¹⁻¹⁴

It ensues that the optical conductivity of a metallic deposit is not perfectly described by Eq. (1). Extra terms must be taken into account, especially those described by $\sigma_{co}(\omega)$ and $\sigma_{sp}(\omega)$ which are conductivities that, respectively, characterize an absorption due to the granular structure of the deposits (collective oscillations of conduction electrons), and an absorption due to surface-roughness effects (surface plasmons).

In spite of the fact that numerous studies have been made of the collective oscillations of conduction electrons in dispersed systems, few results are available for metals which are not either noble or alkali. Moreover, most studies of nonradiative-surface-plasmon excitation are not entirely satisfactory, as few authors have directly measured the parameters: rms surface-roughness heights, and autocorrelation lengths a . With a view to improving this situation, we have undertaken, for magnesium, a static-ultrahigh-vacuum study of the optical properties of granular deposits and rough surfaces.

Transmittance and reflectance measurements of several deposits ranging from approximately 25- to 900-Å thickness were performed under normal incidence and at room temperature, in the energy range 1-6 eV. The structure of the deposits was determined *in situ*, using replication techniques. The discontinuous deposits displayed absorption bands located between 2.5 and 5.12 eV, owing to collective oscillations of conduction electrons. The experimental results with the thinnest deposits have been explained by means of the Maxwell-Garnett¹⁵ and Mie's¹⁶ theories. To explain the shifting of absorption bands to lower energies as the thickness of the deposit increases, the deposits were envisaged as made up of ellipsoidal particles. Continuous rough deposits do not display these absorption bands, but there is a substantial dip in the reflectance at an energy close to that of the surface-plasmon energy. This dip is explained by means

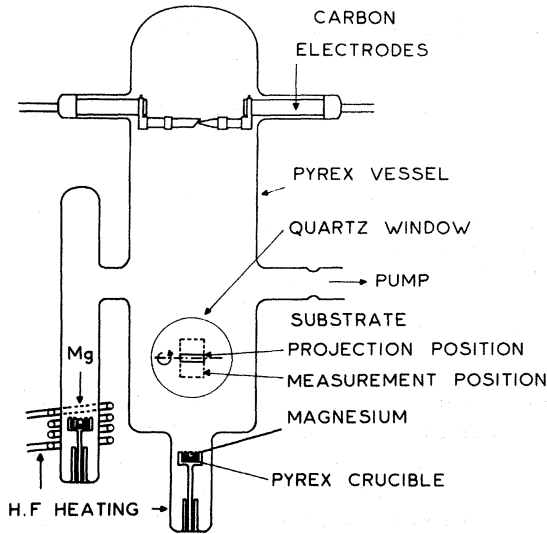


FIG. 1. Diagram of the evaporation device.

of the Elson and Ritchie¹⁷ quantum theory concerning the influence of roughness on scattering.

II. EXPERIMENT

A. Preparation of deposits

The basic apparatus has been described previously.^{18,19} The thin deposits of magnesium were prepared and studied at room temperature, under a static ultrahigh vacuum, i. e., in sealed ampoules in which there is a pressure of about 10^{-9} Torr. The magnesium was placed in a quartz crucible, and purified by high-frequency heating and successive degassing stages. It was condensed on a quartz substrate, 15 mm long, 10 mm wide, and 3 mm thick. Part of the substrate did not receive any metal, and optical measurements were made for comparison. A second crucible was placed in a tube welded to the envelope (Fig. 1). It was used to evaporate magnesium and to deposit, inside the tube, layers that act as a getter. After projection, the substrate was erected by means of magnets, exactly opposite the quartz windows.

B. Photometric measurements

The variations of the transmittance T and reflectance R of deposits versus incident energy $\hbar\omega$ were determined by photometric measurements, by comparing the flux transmitted through and reflected from the thin deposit, with the flux transmitted through and reflected from the transparent substrate. Measurements were performed under normal incidence and in the same vacuum as that used to produce the deposit.

If we assume that the thin deposit is limited by two plane parallel faces separated by a thickness d , and if E_t , E_r , and E_0 designate the complex am-

plitude of the transmitted, reflected, and incident electromagnetic fields, we then obtain, for the passage through the separation areas of the different media,²⁰ the following equations:

$$\frac{E_t}{E_0} = \frac{(1+r_1)(1+r_2)e^{i\tilde{n}\eta}e^{in_s\eta}}{r_1r_2 + e^{2i\tilde{n}\eta}}, \quad (2)$$

$$\frac{E_r}{E_0} = \frac{r_1e^{2i\tilde{n}\eta} + r_2}{r_1r_2 + e^{2i\tilde{n}\eta}}, \quad (3)$$

with $r_1 = (n_0 - n_s)/(n_0 + n_s)$, $r_2 = (\tilde{n} - n_s)/(\tilde{n} + n_s)$, $\eta = 2\pi d/\lambda$. $\tilde{n} = n + ik$ is the complex index of the deposit, d its thickness, n_0 and n_s are, respectively, the index of air and the index of the substrate on which the layer is deposited. The transmittance T and reflectance R are given by

$$T = (n_s/n_0) |E_t/E_0|^2, \quad R = |E_r/E_0|^2.$$

If the thickness d of the deposit is small compared with the wavelength λ , the preceding expressions (2) and (3) can be expanded in a series. By limiting ourselves to the terms in $(d/\lambda)^2$, we obtain²¹

$$2nk\eta = n_s(1 - R - T)/T. \quad (4)$$

If $\epsilon = \epsilon_1 + i\epsilon_2 = \tilde{n}^2$ designates the dielectric constant of the deposit, we obtain

$$\sigma(\omega) = (\omega/4\pi)\epsilon_2 = (n_s c/4\pi d)[(1 - R - T)/T]. \quad (5)$$

Deposits for which $d/\lambda \leq 0.02$ can be studied using this relation.

C. Electron microscopy

Immediately after the optical measurements, the structure of the deposits was determined *in situ*, using the replica technique. A thin layer of carbon was evaporated using two carbon electrodes (Fig. 1). The carbon impression was then removed from the substrate and shadowed with Pt-W at a suitable angle. We encountered some difficulties in obtaining replicas of discontinuous deposits of magnesium. These deposits are made up of closely assembled small grains. We obtained castings which gave their structure accurately when the Pt-W shadow was slight. This is the reason why the photographs of these deposits have a poor contrast. The electron-microscope results should be carefully interpreted. Many experiments are needed before valid conclusions can be obtained. Results, which we give subsequently here, were based on 200 photographs. The electron microscopes used were Philips EM 200 and EM 300.

III. RESULTS AND DISCUSSION

A. Discontinuous deposits

It is difficult to prepare discontinuous deposits of magnesium, as they soon become continuous.

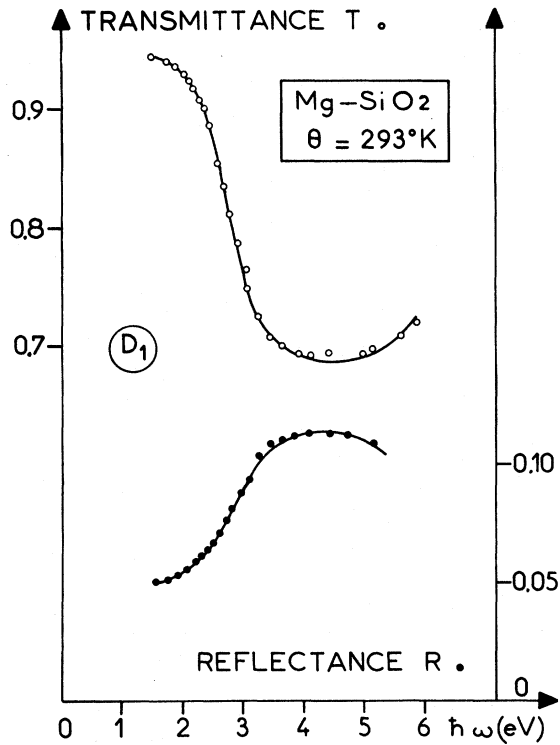


FIG. 2. Transmittance and reflectance vs incident energy for deposit D_1 (thickness $d \sim 50 \text{ \AA}$).

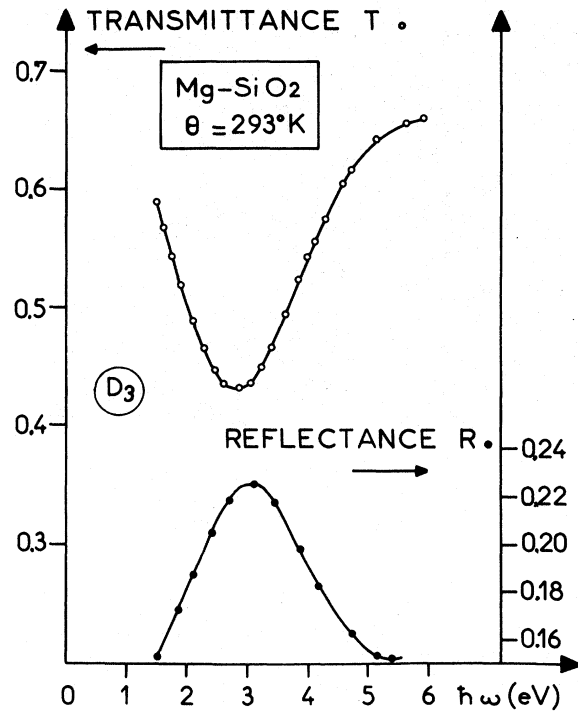


FIG. 4. Transmittance and reflectance vs incident energy for deposit D_3 (thickness $d \sim 120 \text{ \AA}$).

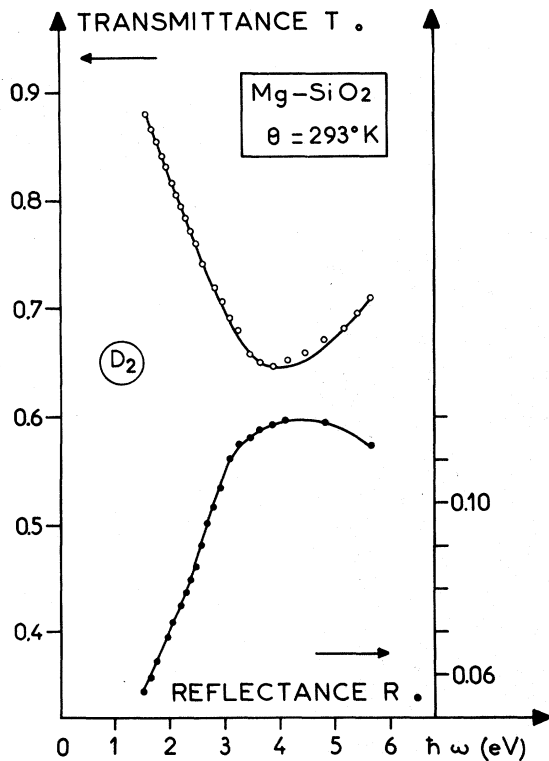


FIG. 3. Transmittance and reflectance vs incident energy for deposit D_2 (thickness $d \sim 70 \text{ \AA}$).

Figures 2-4 give the variations of the transmittance T and reflectance R versus incident energy $\hbar\omega$ for three deposits, D_1 , D_2 , D_3 , of thicknesses approximately 50, 70, and 120 \AA . The thinnest deposit is made up of small spherical and semi-spherical grains (Fig. 5), and at a subsequent stage, these fuse together giving larger grains

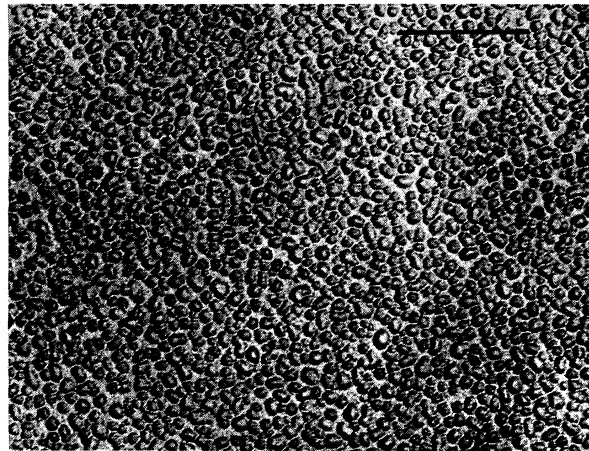


FIG. 5. Carbon replica made under static ultrahigh vacuum of deposit D_1 . Platinum shadow casting at an angle of 50° . The line represents $0.2 \mu\text{m}$.

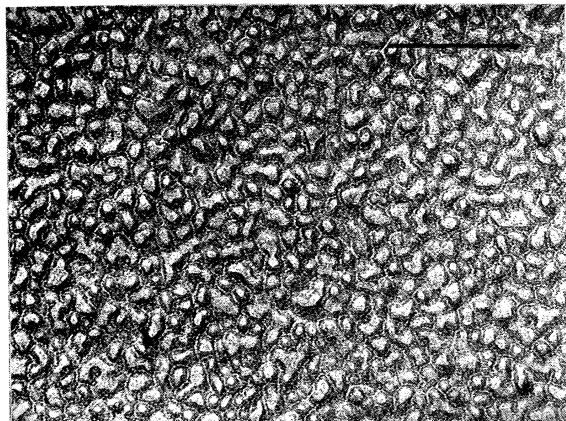


FIG. 6. Carbon replica made under static ultrahigh vacuum of deposit D_2 . Platinum shadow casting at an angle of 50° . The line represents $0.2 \mu\text{m}$.

(Figs. 6 and 7), which look like irregularly shaped and closely spaced puddles. The volume fraction of the metal q is equal to 0.4 for D_1 , 0.58 for D_2 , and 0.60 for D_3 . Figures 2–4 show damped resonance peaks in R and T . These peaks shift to lower energies as the thickness of the deposit is increased. When the thickness of deposit approaches zero, the resonance energy tends to a value that can be determined. Figure 8 gives the variations of transmittance T versus incident energy, for deposits D_3 , D'' , D' of decreasing thickness (120, 80, 25 Å) prepared under very similar conditions. The locus of the minima of T is a regular curve, plotted as a dashed line in Fig. 8, which meets the transmission curve of the transparent substrate (approaching a zero deposit) for $\hbar\omega_r = 5.12 \text{ eV}$.

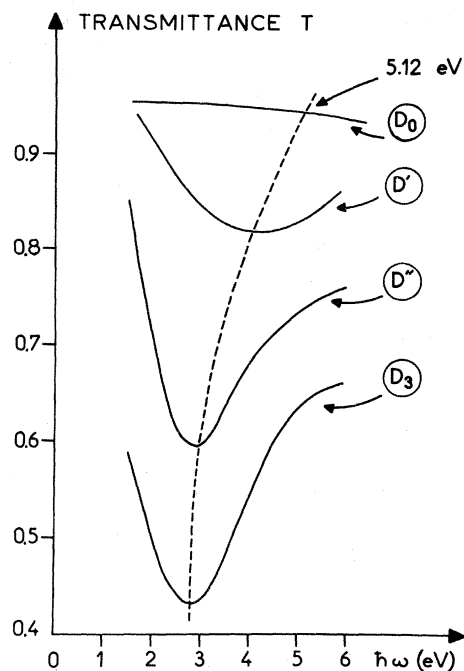


FIG. 8. Transmittance vs incident energy for three deposits D' ($\sim 25 \text{ \AA}$), D'' ($\sim 80 \text{ \AA}$), D_3 ($\sim 120 \text{ \AA}$) prepared under very similar conditions. D_0 is the transmittance of the substrate.

Figure 9 gives the variations—for deposits D_1 , D_2 , and D_3 —of the optical conductivity $\sigma(\omega)$ versus incident energy $\hbar\omega$, evaluated according to the approximate formula (5). There are absorption bands respectively located at 4.8, 4.2, and 2.8 eV. These bands do not occur with bulk metal. Magnesium is a nearly-free-electron metal and its dielectric con-

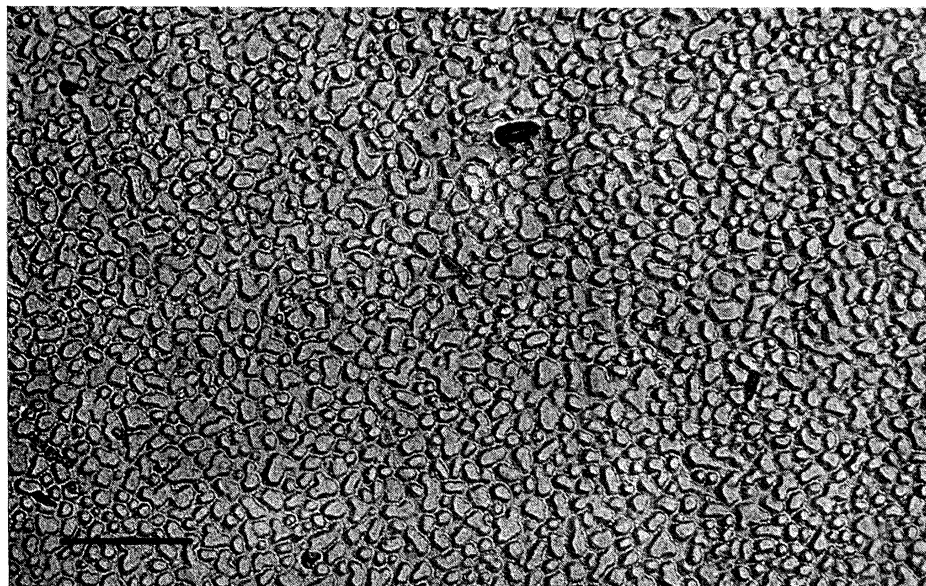


FIG. 7. Carbon replica made under static ultrahigh vacuum of deposit D_3 . Platinum shadow casting at an angle of 50° . The line represents $0.2 \mu\text{m}$.

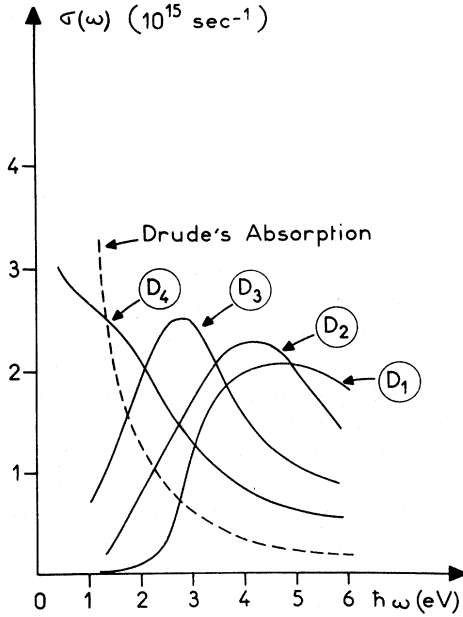


FIG. 9. Optical conductivity vs incident energy for deposits D_1 , D_2 , D_3 , and D_4 .

stant is given by

$$\epsilon = \epsilon_1 + i\epsilon_2 = 1 - \frac{\omega_p^2}{\omega^2 + \gamma^2} + i \frac{\gamma}{\omega} \frac{\omega_p^2}{\omega^2 + \gamma^2}, \quad (6)$$

where the plasma energy $\hbar\omega_p$ and the damping term $\hbar\gamma$ are respectively set equal to 10.5 and 0.4 eV. The optical conductivity of bulk metal, $\sigma_D(\omega) = (\omega/4\pi)\epsilon_2$, plotted as a dashed line in Fig. 9, is quite different from the conductivity of thin deposits. These deposits display absorption peaks and Drude's absorption no longer exists. These peaks are due to collective oscillations of conduction electrons in metallic grains of magnesium. The interaction of a plane electromagnetic wave with spherical particles embedded in a transparent medium was first thoroughly discussed by Maxwell-Garnett¹⁵ and Mie.¹⁶ According to Maxwell-Garnett's theory the physical system is generally composed of a dielectric matrix in which the metal aggregates are dispersed, and may thus be specified phenomenologically by its complex and frequency-dependent dielectric constant $\epsilon_d(\omega) = \epsilon_{1d}(\omega) + i\epsilon_{2d}(\omega)$. The optical properties of aggregated metal systems may be described in terms of the dielectric constant of the dielectric matrix ϵ_0 , the frequency-dependent and complex dielectric constant of the metal aggregates, $\epsilon(\omega) = \epsilon_1(\omega) + i\epsilon_2(\omega)$, and the volume fraction of the metal q , by means of the following relation:

$$(\epsilon_d - \epsilon_0)/(\epsilon_d + 2\epsilon_0) = q(\epsilon - \epsilon_0)/(\epsilon + 2\epsilon_0). \quad (7)$$

It is assumed that the metal aggregates are spheri-

cal, much smaller than the wavelength of the incident light, and randomly distributed in the dielectric matrix. The size of the individual metal spheres is irrelevant as long as it is much less than the wavelength of the incident light. Marton and Lemon²² have shown that this theory gives a good qualitative description of the optical properties of aggregated systems for all values of q , when $0 < q < 1$, but not for $q=0$ and $q=1$. By separating the imaginary and real parts of relation (7), the following formula may be obtained when q is small:

$$\sigma_d(\omega) = \frac{\omega}{4\pi} \epsilon_{2d} = A \frac{\omega \epsilon_2}{(\epsilon_1 + B\epsilon_0)^2 + \epsilon_2^2}, \quad (8)$$

with $A = 9q\epsilon_0^2/4\pi(1-q)^2$ and $B = (2+q)/(1-q)$. The spectrum of $\sigma_d(\omega)$ shows a maximum absorption at or near $\epsilon_1 = -B\epsilon_0$, which shifts to smaller energies as particle packing increases. By inserting the value $\epsilon = \epsilon_1 + i\epsilon_2$ given by Eq. (6) into Eq. (8) (with $\hbar^2\omega^2 \gg \hbar^2\gamma^2$), we obtain a Lorentzian form with a peak when the frequency is such that

$$\omega_r = \omega_p(1 + B\epsilon_0)^{-1/2}. \quad (9)$$

When q approaches zero,

$$\omega_r = \omega_p(1 + 2\epsilon_0)^{-1/2}. \quad (10)$$

This formula was also obtained by Doyle,² using the zero-size limit of Mie's theory and the free-electron model. For particles in a thin layer deposited on a dielectric substrate of refractive index n_s , there is some doubt as to the proper value of ϵ_0 to be used in Eq. (10). According to the studies of Yoshida *et al.*,⁷ $\epsilon_0 = n_s^2$. Equation (10) then gives $\hbar\omega_r = 4.96$ eV, in good agreement with experimental results ($\hbar\omega_r = 5.12$ eV). It should be pointed out that our results are also in agreement with those obtained on finely dispersed magnesium colloidal centers.²³ Experimental results on thicker deposits cannot be explained in terms of the Maxwell-Garnett and Mie theories. Deposits D_2 and D_3 which have approximately the same volume fraction of metal q display absorption bands located at two different energy values. The theory should be improved by means of experimental models. In Figs. 6 and 7 it is shown that thin deposits are generally composed of "islands" resembling liquid drops. The optical properties of such granular deposits can be characterized using simple analytic formulas, if it is assumed that the metal particles have ellipsoidal shapes and that they are surrounded everywhere by a medium of given dielectric constant ϵ_0 . David,²⁴ Schopper,²⁵ Galeener,²⁶ and Meessen²⁷ have proposed a simple method for treating the case of aligned ellipsoidal particles with direction of polarization parallel to a principal axis of an ellipsoid. The following formula gives the conductivity of such a deposit:

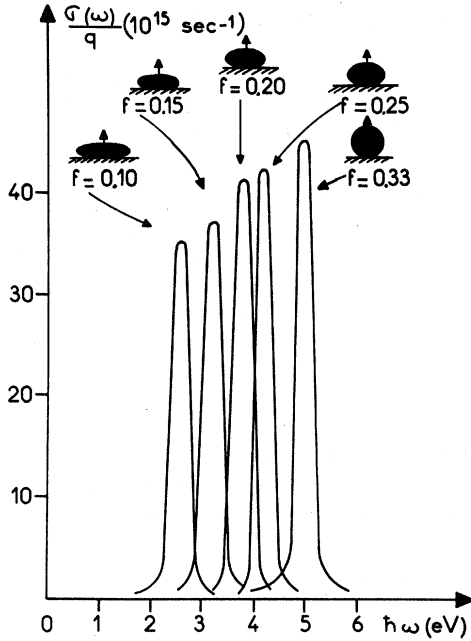


FIG. 10. Frequency dependence of optical conductivity of an aggregated system for various forms of particles. Curves were calculated from Eq. (11) with ϵ_1 and ϵ_2 given by Eq. (6).

$$\sigma(\omega) = \frac{q}{4\pi} \frac{\epsilon_2 \omega}{[1 + (\epsilon_1 - \epsilon_0)f/\epsilon_0]^2 + (\epsilon_2 f/\epsilon_0)^2} \quad (11)$$

as shown in the Appendix. The ellipsoidal particles are assumed to be axially symmetrical, so that they have circular cross sections in the plane of the deposit. q is the volume fraction of the metal; f is a "form" factor which depends on the axis ratio of the ellipsoids (f is equal to $\frac{1}{3}$ for a sphere and its value increases with decreasing dimensions of the metal particles along the applied field); ϵ_0 is the numerical average of the dielectric constants of the substrate and air, namely, $\epsilon_0 = \frac{1}{2}(1 + n_s^2)$; the dielectric constant of the particles is the same as that of the bulk metal. The simple equation (11) is only valid when the lateral interactions among the metal particles are negligible. To obtain a more general expression, one must also consider the effect of the secondary electric field, which is created by the dipoles induced in the metal particles. By considering separately the two cases where the dipoles are oriented in a direction parallel or perpendicular to the plane of the deposit, Meessen²⁷ has shown that the lateral interactions among the metal grains have the sole effect of changing the "form" factor. This effect will therefore not be taken into account here. Discontinuous deposits of noble metals have already been studied by means of Eq. (11).^{28,29} By inserting the value of $\epsilon = \epsilon_1 + i\epsilon_2$ given by Eq. (6) into Eq. (11) (with $\hbar^2\omega^2$

$\gg \hbar^2\gamma^2$), we obtain a Lorentzian form with a peak at a frequency

$$\omega_r = \omega_p [1 + \epsilon_0(1/f - 1)]^{-1/2}. \quad (12)$$

It should be pointed out that $f = \frac{1}{3}$, this again gives Eq. (10). With a continuous foil ($f=1$, $q=1$, $\epsilon_0=1$), Eq. (11) gives a quantity proportional to the energy-loss function³⁰

$$\sigma(\omega) \propto \epsilon_2 / (\epsilon_1^2 + \epsilon_2^2) = \text{Im}(\epsilon^{-1}). \quad (13)$$

Equation (11) may be considered as a generalization of the energy-loss function for particles of different forms, and surrounded by a medium of dielectric constant ϵ_0 . Equation (11) displays a series of peaks for different values of f , i.e., for different particle shapes. Some of these peaks are given in Fig. 10. It is seen that the peak for a sphere is located at a higher energy than the peak for a flat disk. This is borne out by our experiments. The position and the large damping of absorption bands can be explained, taking into account that a thin deposit is made up of all sorts of particles with different axis ratios. It should also be pointed out that

$$\sigma(\omega)_{\text{max}} = \frac{q}{4\pi f^2} \left(\frac{\omega \epsilon_0^2}{\epsilon_2} \right)_{\omega=\omega_r},$$

i.e., the peak is particularly strong when the resonance occurs in the frequency range where the bulk metal has a low absorption (small ϵ_2). It is for this reason that dispersed systems of noble and alkali metals (for which ϵ_2 is small in the visible frequency range), show spectacular effects.^{3,29} Moreover, in the low-frequency limit ($\omega \ll \omega_p$), it follows from Eq. (11) that $\sigma(\omega)$ is close to zero. The discontinuous deposit becomes completely transparent in the infrared frequency range, although the metal forming the deposit displays a very strong Drude's absorption in this frequency range. This was confirmed by experiment (Fig. 9).

B. Continuous rough deposits

Figure 11 gives the variations of the transmittance T and reflectance R versus incident energy $\hbar\omega$, for deposit D_4 of approximately 160-Å thickness. This deposit is not totally opaque and displays surface roughness (Fig. 12). There is no longer any resonance. However, as can be seen in Fig. 9, the absorption of this deposit is greater than that evaluated according to free-electron theory. The optical conductivity of this deposit results from Drude's term $\sigma_D(\omega)$, and also from an additional term characterizing its disordered structure. If we subtract Drude's term from the experimentally observed optical conductivity, an absorption band may be observed of the same kind as that found on the discontinuous deposit.³¹ Figure 13 shows the variations of the reflectance R versus

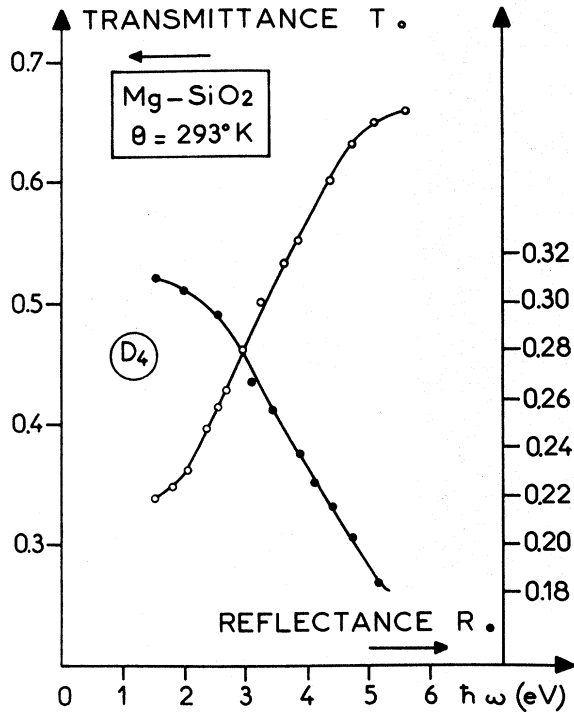


FIG. 11. Transmittance and reflectance vs incident energy for deposit D_4 (thickness $d \sim 160 \text{ \AA}$).

incident energy $\hbar\omega$ for deposit D_5 , which is approximately 500 \AA thick and totally opaque. Reflectance decreases towards high energies. This conspicuous dip, which is in agreement with the data of Gesell *et al.*¹³ and Daudé *et al.*,¹⁴ occurs at an energy close to that of the surface-plasmon energy

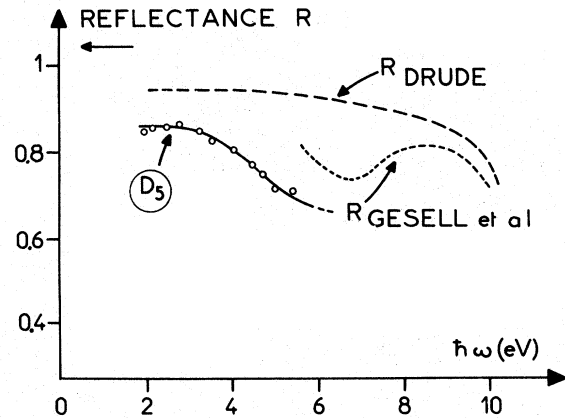


FIG. 13. Reflectance vs incident energy for deposit D_5 (thickness $d \sim 500 \text{ \AA}$, totally opaque). R_{Drude} is the reflectance calculated assuming a Drude model for a nearly free electron metal with ϵ given by Eq. (6). R_{Gesell} represents Gesell *et al.*¹³ measurements.

for magnesium, $\hbar\omega_s = \hbar\omega_p/\sqrt{2} = 7.4 \text{ eV}$. A carbon replica of this deposit (Fig. 14) shows substantial surface roughness. Figure 14 also shows that the surface is regular enough to be characterized by the parameters describing the interaction between an incident plane wave and the surface. These parameters are the rms surface-roughness heights δ and autocorrelation length a . The existence of a reflectance minimum in the energy range of the surface plasmons can be explained by surface roughness, which gives scattering and resonant coupling between the electric field of the incident wave and the surface plasmons. A quantum theory

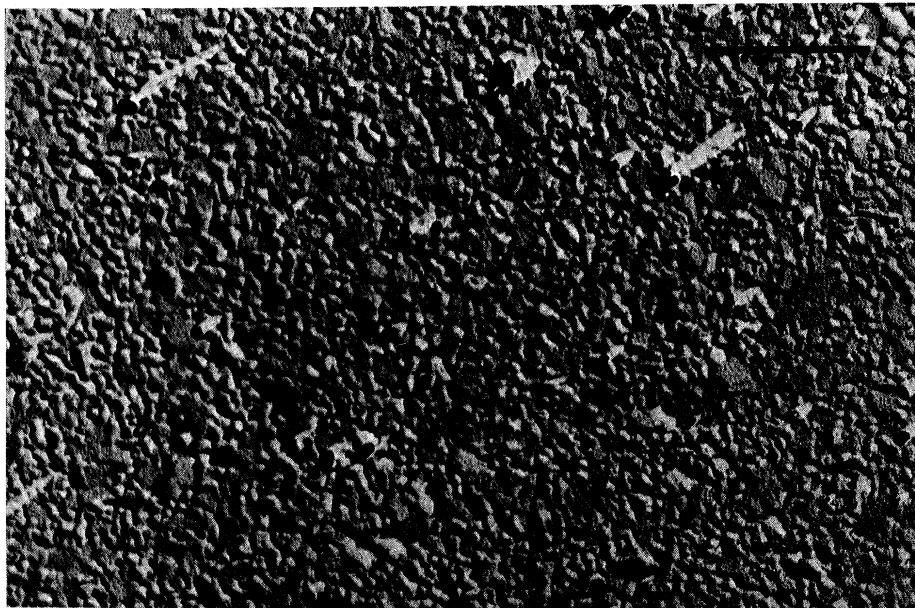


FIG. 12. Carbon replica made under static ultrahigh vacuum of deposit D_4 . Platinum shadow casting at an angle of 70° . The line represents $0.5 \mu\text{m}$.

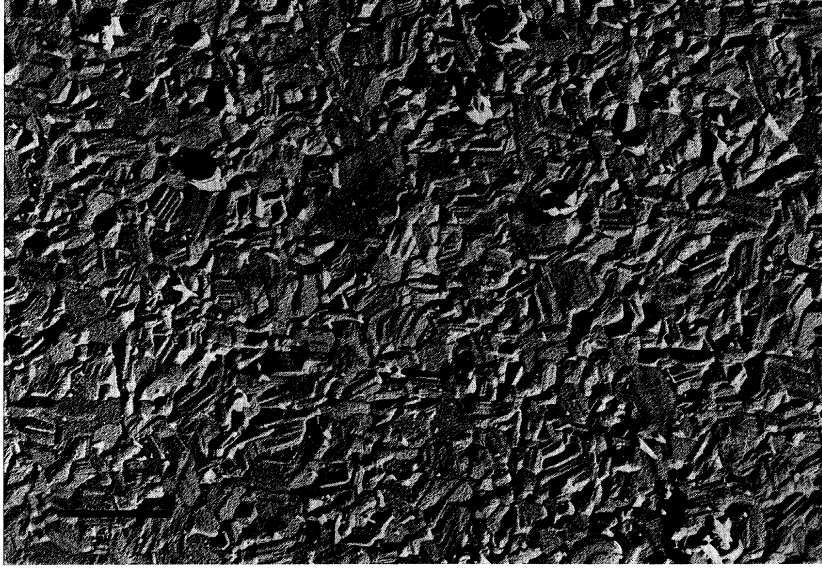


FIG. 14. Carbon replica made under static ultrahigh vacuum of deposit D_5 . Platinum shadow casting at an angle of 70° . The line represents $1 \mu\text{m}$.

of the influence of roughness on scattering has been proposed by Elson and Ritchie.¹⁷ These authors used first-order perturbation theory to evaluate the scattering and conversion to surface-plasma oscillations of photons normally incident on a nearly planar vacuum-dielectric surface. The probability that a photon normally incident on a rough metallic surface will create a surface plasmon may be expressed as the decrease in reflectance of the specular beam, viz.,¹⁷

$$\Delta R_{sp} = \delta^2 (\omega/c)^4 \{ \epsilon_1^2 / [- (1 + \epsilon_1)]^{5/2} \} g(k). \quad (14)$$

δ is the rms surface roughness height of the metal surface, and $g(k)$ is the Fourier transform of the autocorrelation function. The wave number k is related to ω by the surface-plasmon dispersion relation

$$k = (\omega/c) [\epsilon_1 / (1 + \epsilon_1)]^{1/2}. \quad (15)$$

By inserting in Eq. (14) the value of ϵ_1 given by (6) (with $\hbar^2 \omega^2 \gg \hbar^2 \gamma^2$), the expression for ΔR_{sp} is reduced to¹⁷

$$\Delta R_{sp} = \delta^2 (\omega_p/c)^4 (1 - \alpha^2)^{-1/2} \gamma^5 g(\gamma \omega_p/c), \quad (16)$$

where

$$\alpha = \omega/\omega_p, \quad \gamma = \alpha [(1 - \alpha^2) / (1 - 2\alpha^2)]^{1/2}.$$

Elson and Ritchie have also calculated the diffuse scattering for photons normally incident on a rough metallic surface. For s and p polarized scattered light, they obtained the differential scattering probabilities given by

$$\frac{dP_s}{d\Omega} = \left(\frac{\delta}{\pi} \right)^2 \left(\frac{\omega}{c} \right)^4 \cos^2 \theta \sin^2 \varphi g(k), \quad (17)$$

$$\begin{aligned} \frac{dP_p}{d\Omega} &= \left(\frac{\delta}{\pi} \right)^2 \left(\frac{\omega}{c} \right)^4 \cos^2 \theta \cos^2 \varphi \\ &\times \frac{\sin^2 \theta - \epsilon_1}{\sin^2 \theta - \epsilon_1 \cos^2 \theta} g(k), \end{aligned} \quad (18)$$

where φ is the azimuthal angle, θ is the polar angle, Ω is the solid angle, and the dispersion relation for k is given by

$$k = (\omega/c) \sin \theta. \quad (19)$$

Gesell *et al.*¹³ have recently used this theory to explain the results of their experiments. They assumed an autocorrelation function of Gaussian form

$$g(k) = \pi a^2 e^{-(a^2 k^2/4)} \quad (20)$$

where a is the autocorrelation length. With a deposit 450 \AA thick they found $a = 275 \text{ \AA}$ and $\delta = 36 \text{ \AA}$. Using Fig. 14 for a direct measurement, we found $\delta = 60 \text{ \AA}$. The deposit D_5 which we studied was rougher than the film studied by Gesell *et al.* and the thickness was approximately equivalent. This is further confirmed by the fact that the decrease in reflectance is greater in our experiments than in theirs.

Until now we have not been able to carry out further investigations of the theory, because with our apparatus we cannot obtain reflectance measurements beyond 6 eV . We have verified that the roughness of magnesium deposits increases with thickness. Braundmeier *et al.*³² found the same effect with aluminum. In Figs. 15 and 16, carbon replicas of a magnesium deposit (900 \AA) are given at two different magnifications, and there is very substantial surface roughness. These photographs reveal the growth characteristics of magnesium de-

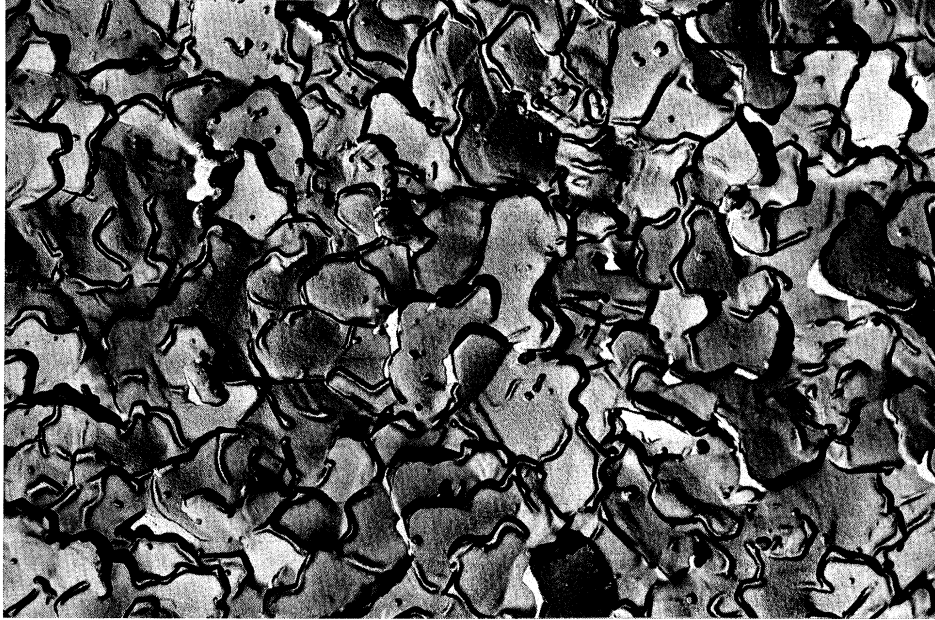


FIG. 15. Carbon replica made under static ultrahigh vacuum of a totally opaque deposit of magnesium ($d \sim 900 \text{ \AA}$). Platinum shadow casting at an angle of 60° . The line represents $1 \mu\text{m}$.

posits. This kind of structure had already been found by Rhodin.³³

IV. CONCLUSION

Discontinuous deposits of magnesium show absorption bands, owing to collective oscillations of conduction electrons, which have the same characteristics as those of noble and alkali metals.^{3,8} It would be very interesting to prepare deposits with a slight volume fraction of metal, and typically shaped grains. Structural models could thus be used allowing improved verification of the theory. The dip in reflectance on rough deposits can be interpreted in terms of absorption due to excitation

of nonradiative surface plasmons. We feel that a more complete check of Elson and Ritchie's theory could be effected by preparing deposits at low temperature (under such conditions deposits are less rough), and using Dobberstein's³⁴ method to determine the exact shape of the autocorrelation function. The results of these investigations will be published later on.

APPENDIX

Let us consider an ideal deposit composed of ellipsoidal particles assumed to be axially symmetrical, so that they have circular cross sections in the plane of the deposit. The applied field polar-

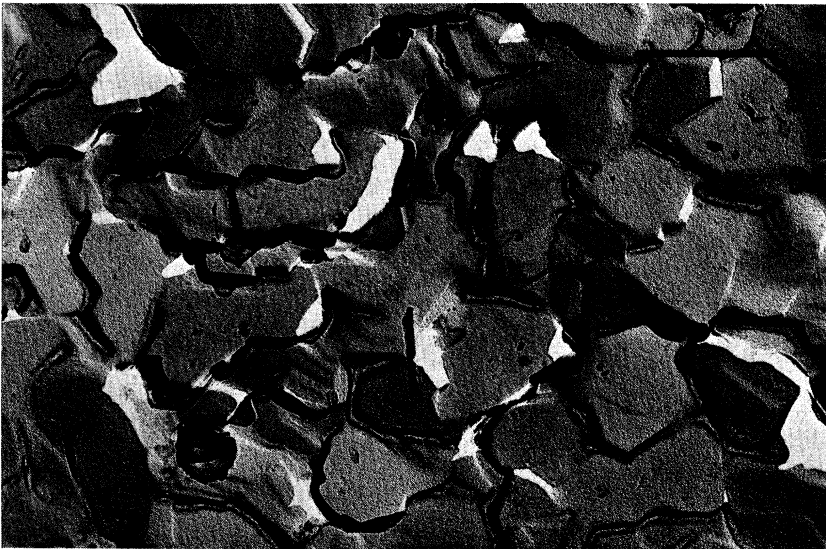


FIG. 16. Carbon replica of deposit shown in Fig. 15 with different magnification. The line represents $0.5 \mu\text{m}$.

izes the material of the metal particle, and induces a surface charge of opposite sign on the two surfaces which delimit the material particle in the direction of the applied field. Assuming at first that the metal particle is surrounded by vacuum, the surface charge depends solely on the polarization density \vec{P} within the metal grain, and the particular shape of this grain. The induced surface charges create a "depolarizing field" \vec{E}' such as

$$\vec{P} = \alpha(\vec{E} + \vec{E}'), \quad (21)$$

where α is the polarizability of the material. When the shape of the metal particle is relatively symmetrical along the applied field, we can assume that

$$\vec{E}' = -D\vec{P}, \quad (22)$$

where D is the "depolarization factor." The three components of D along the three main axis of the ellipsoid agree with the relation

$$D_x + D_y + D_z = 4\pi. \quad (23)$$

Let us introduce a "form factor" f using the relation

$$\vec{E}' = -4\pi f\vec{P}, \quad (24)$$

so that the components of f agree with the sum rule

$$f_x + f_y + f_z = 1. \quad (25)$$

f depends on the ratio of the ellipsoid axis (f is equal to $\frac{1}{3}$ for a sphere, and its value increases with decreasing dimensions of the metal particle along the applied field). Relations (21) and (24)

give

$$\vec{P} = \frac{1}{4\pi} \left(\frac{\epsilon - 1}{1 + (\epsilon - 1)f} \right) \vec{E} = \alpha' \vec{E}, \quad (26)$$

where $\epsilon = 1 + 4\pi\alpha$ is the dielectric constant of the material that constitutes the metal particle.

Let us now assume that the ellipsoid is surrounded by a medium of dielectric constant ϵ_0 , the numerical average of the dielectric constants of the substrate and air, namely, $\epsilon_0 = \frac{1}{2}(1 + n_0^2)$. When the incident field is parallel to the x axis ($P = P_x$, $f = f_x$), solving the equations for the electrostatic potential with adequate boundary conditions shows that (26) can be replaced by

$$P = \alpha' E = \frac{1}{4\pi} \frac{\epsilon - \epsilon_0}{1 + (\epsilon/\epsilon_0 - 1)f}. \quad (27)$$

The dielectric constant ϵ_d of the deposit which is made up of N identical particles per unit of volume is given by

$$\epsilon_d = \epsilon_0 + 4\pi NV\alpha' = \epsilon_0 + q \frac{\epsilon - \epsilon_0}{1 + (\epsilon/\epsilon_0 - 1)f}, \quad (28)$$

where V is the volume of a particle, $q = NV$ is the volume fraction of the metal, and $\epsilon_d = \epsilon_{1d} + i\epsilon_{2d}$. Finally, we obtain the conductivity of the deposit

$$\sigma(\omega) = \frac{\epsilon_{2d}\omega}{4\pi} = \frac{q}{4\pi} \frac{\omega\epsilon_2}{[1 + (\epsilon_1 - \epsilon_0)f/\epsilon_0]^2 + (\epsilon_2 f/\epsilon_0)^2}.$$

ACKNOWLEDGMENTS

The authors wish to express their gratitude to N. J. C. Boord and J. P. Isaia for translating their text.

¹R. W. Wood, *Philos. Mag.* **3**, 396 (1902).

²W. T. Doyle, *Phys. Rev.* **111**, 1067 (1958); W. T. Doyle and A. Agarwal, *J. Opt. Soc. Am.* **55**, 305 (1965).

³G. Rasigni and P. Rouard, *J. Opt. Soc. Am.* **53**, 604 (1963).

⁴R. H. Doremus, *J. Appl. Phys.* **37**, 2775 (1966).

⁵R. Payan, *Ann. Phys. (Paris)* **4**, 543 (1969).

⁶I. S. Radchenko, *Fiz. Tverd. Tela* **11**, 1829 (1969) [*Sov. Phys.-Solid State* **11**, 1476 (1970)].

⁷J. Yoshida, T. Yamaguchi, and A. Kinbara, *J. Opt. Soc. Am.* **62**, 1415 (1972).

⁸M. Rasigni and G. Rasigni, *J. Opt. Soc. Am.* **63**, 775 (1973).

⁹R. W. Cohen, G. D. Cody, M. D. Coutts, and B. Abeles, *Phys. Rev. B* **8**, 3689 (1973).

¹⁰W. Steinmann, *Phys. Status Solidi* **28**, 437 (1968).

¹¹J. L. Stanford, H. E. Bennett, E. J. Ashley, and E. T. Arakawa, *Bull. Am. Phys. Soc.* **13**, 989 (1968).

¹²J. G. Endriz and W. E. Spicer, *Phys. Rev. B* **4**, 4144 (1971).

¹³T. F. Gesell, E. T. Arakawa, M. W. Williams, and R. N. Hamm, *Phys. Rev. B* **7**, 5141 (1973).

¹⁴A. Daudé, A. Savary, and S. Robin, *J. Opt. Soc. Am.* **62**, 1 (1972).

¹⁵J. C. Maxwell-Garnett, *Philos. Trans. R. Soc. Lond.* **203**, 385 (1904); **205**, 237 (1906).

¹⁶G. Mie, *Ann. Phys. (Leipz.)* **25**, 377 (1908).

¹⁷J. M. Elson and R. N. Ritchie, *Phys. Status Solidi B* **62**, 461 (1974).

¹⁸J. P. Petrakian and J. P. Palmari, *Thin Solid Films* **4**, 423 (1969).

¹⁹M. Rasigni and G. Rasigni, *J. Opt. Soc. Am.* **62**, 1033 (1972).

²⁰O. S. Heavens, *Optical Properties of Thin Solid Films* (Butterworths, London, 1965).

²¹H. Wolter, *Z. Phys.* **113**, 547 (1939).

²²J. P. Marton and J. R. Lemon, *Phys. Rev. B* **4**, 271 (1971); *J. Appl. Phys.* **44**, 3953 (1973).

²³K. K. Shvarts, A. F. Lyushina, and A. Y. Vitol, *Fiz. Tverd. Tela* **11**, 1885 (1969) [*Sov. Phys.-Solid State* **11**, 1519 (1970)].

²⁴E. David, *Z. Phys.* **105**, 269 (1937).

²⁵H. Schopper, *Z. Phys.* **130**, 565 (1951).

²⁶F. L. Galeener, *Phys. Rev.* **27**, 421 (1971); **27**, 1716 (1971).

²⁷A. Meessen, *J. Phys. (Paris)* **33**, 371 (1972).

²⁸G. Rasigni, *Rev. Opt. Theor. Inst.* **41**, 615 (1962).

²⁹A. Emeric and N. Emeric, *Thin Solid Films* **1**, 13 (1967).

³⁰H. Fröhlich and H. Pelzer, *Proc. Phys. Soc. Lond.* **A 68**, 525 (1953).

³¹Deposit D_4 was not totally opaque. The Drude term can-

not be wholly taken into account, so that it is impossible to execute this construction.

- ³²A. J. Braundmeier, M. W. Williams, E. T. Arakawa, and R. H. Ritchie, *Phys. Rev. B* 5, 2754 (1972).
- ³³T. N. Rhodin, *Structure and Properties of Thin Films*, edited by C. A. Neugabauer, J. B. Newkirk, and D. A. Verlilyea (Wiley, New York, London, 1959), p. 87.
- ³⁴P. Dobberstein, *Phys. Lett. A* 31, 307 (1970).

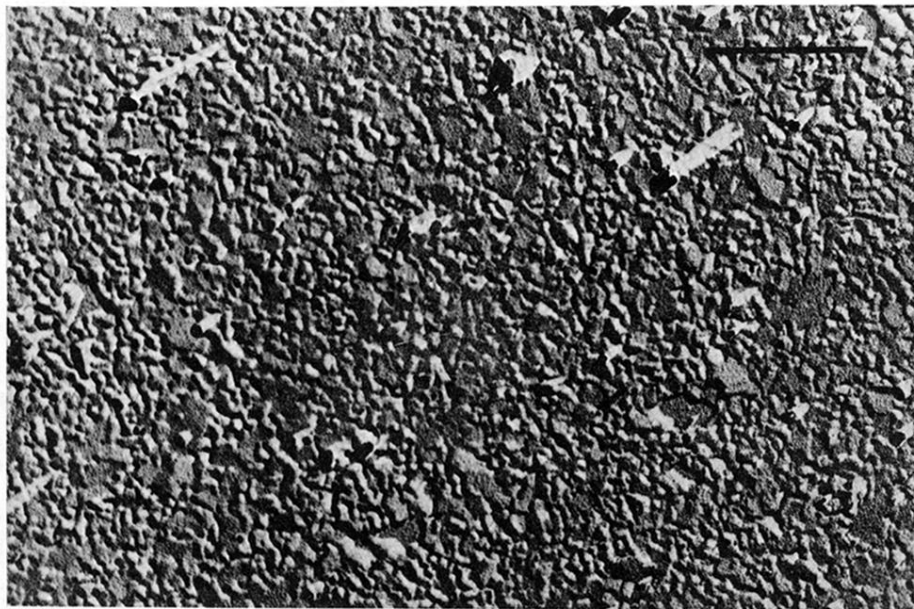


FIG. 12. Carbon replica made under static ultrahigh vacuum of deposit D_4 . Platinum shadow casting at an angle of 70° . The line represents $0.5 \mu\text{m}$.

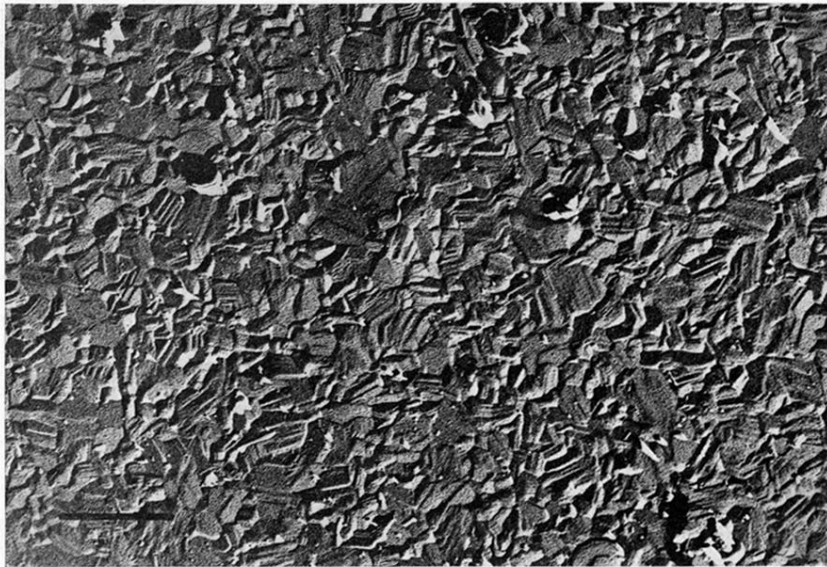


FIG. 14. Carbon replica made under static ultrahigh vacuum of deposit D_5 . Platinum shadow casting at an angle of 70° . The line represents $1 \mu\text{m}$.

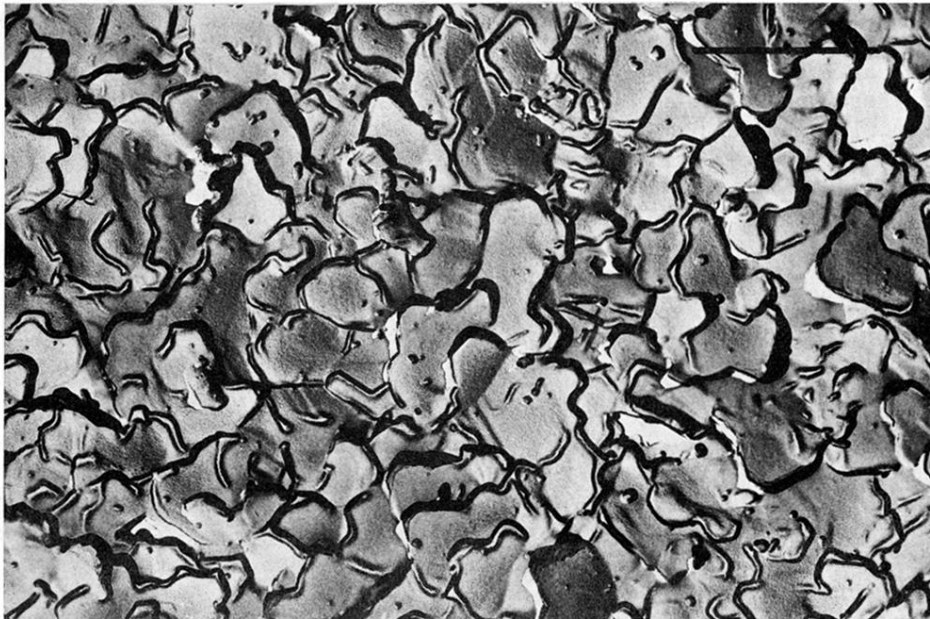


FIG. 15. Carbon replica made under static ultrahigh vacuum of a totally opaque deposit of magnesium ($d \sim 900 \text{ \AA}$). Platinum shadow casting at an angle of 60° . The line represents $1 \mu\text{m}$.

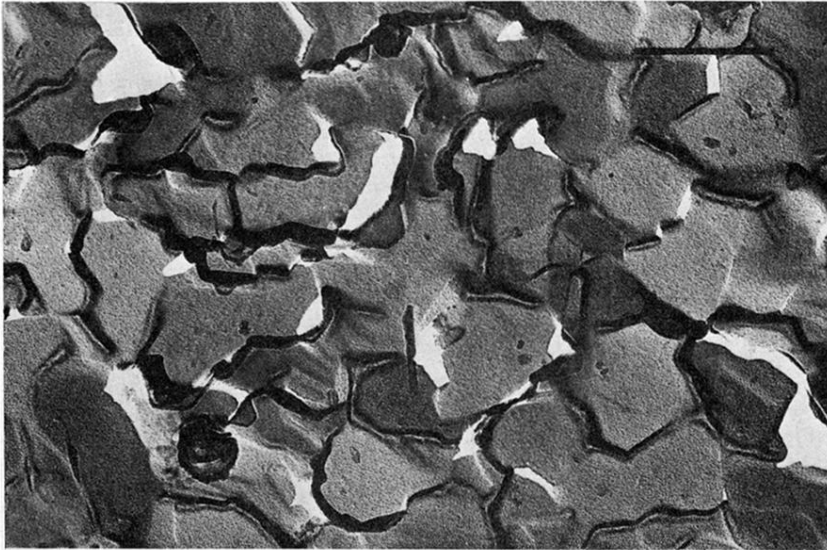


FIG. 16. Carbon replica of deposit shown in Fig. 15 with different magnification. The line represents $0.5 \mu\text{m}$.

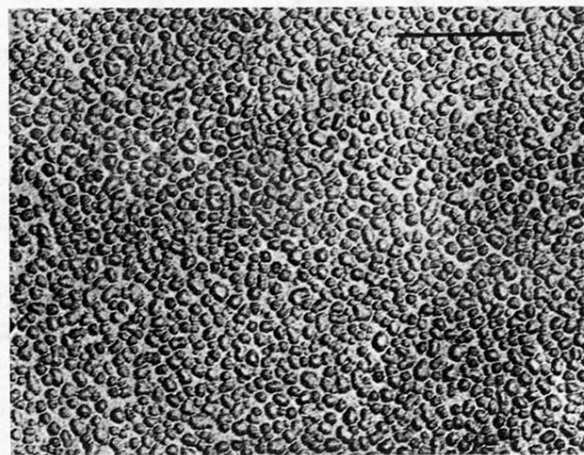


FIG. 5. Carbon replica made under static ultrahigh vacuum of deposit D_1 . Platinum shadow casting at an angle of 50° . The line represents $0.2 \mu\text{m}$.

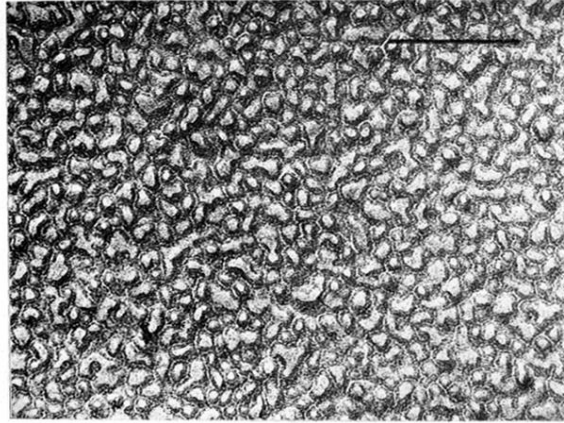


FIG. 6. Carbon replica made under static ultrahigh vacuum of deposit D_2 . Platinum shadow casting at an angle of 50° . The line represents $0.2 \mu\text{m}$.

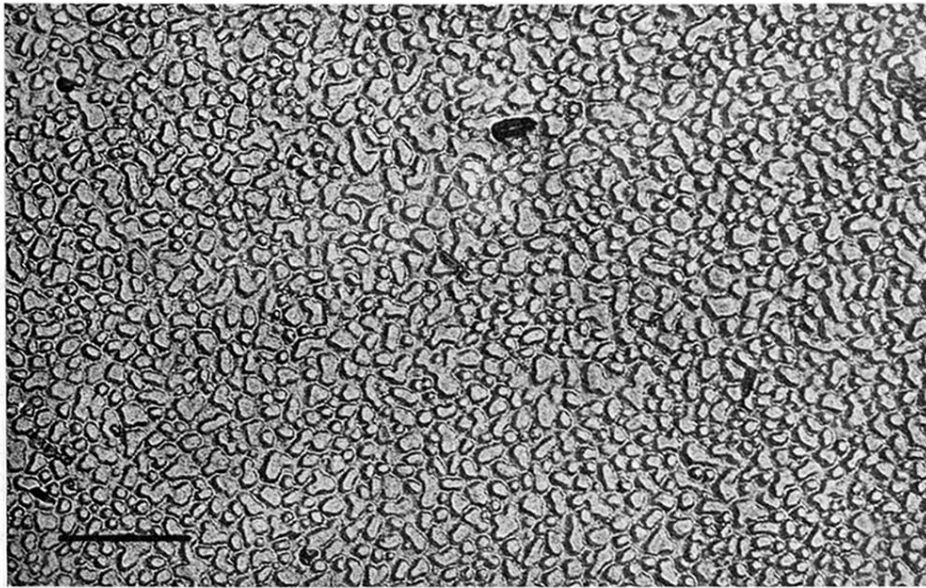


FIG. 7. Carbon replica made under static ultra-high vacuum of deposit D_3 . Platinum shadow casting at an angle of 50° . The line represents $0.2 \mu\text{m}$.